Mon. Not. R. Astron. Soc. **350,** 1301–1309 (2004) doi:10.1111/j.1365-2966.2004.07713.x

The single-degenerate channel for the progenitors of Type Ia supernovae

Z. Han[1]★ and Ph. Podsiadlowski[2]

[1]*National Astronomical Observatories/Yunnan Observatory, the Chinese Academy of Sciences, PO Box 110, Kunming 650011, China*
[2]*University of Oxford, Department of Astrophysics, Keble Road, Oxford OX1 3RH*

Accepted 2004 February 10. Received 2004 February 9; in original form 2003 September 23

ABSTRACT

We have carried out a detailed study of one of the most favoured evolutionary channels for the production of Type Ia supernova (SN Ia) progenitors, the single-degenerate channel (CO + MS), where a carbon/oxygen (CO) white dwarf (WD) accretes matter from an unevolved or slightly evolved non-degenerate star until it reaches the Chandrasekhar mass limit. Employing Eggleton's stellar evolution code and adopting the prescription of Hachisu et al. for the accretion efficiency, we performed binary stellar evolution calculations for about 2300 close WD binary systems and mapped out the initial parameters in the orbital period–secondary mass (P–M_2) plane (for a range of WD masses) which lead to a successful Type Ia supernova. We obtained accurate, analytical fitting formulae to describe this parameter range which can be used for binary population synthesis (BPS) studies. The contours in the P–M_2 plane differ from those obtained by Hachisu et al. for low-mass CO WDs, which are more common than massive CO WDs. We confirm that WDs with a mass as low as 0.67 $M_\odot$ can accrete efficiently and reach the Chandrasekhar limit. We have implemented these results in a BPS study to obtain the birth rates for SNe Ia and the evolution of birth rates with time of SNe Ia for both a constant star formation rate and a single starburst. The birth rates are lower than (but comparable to) those inferred observationally.

Key words: binaries: close – stars: evolution – supernovae: general – white dwarfs.

Downloaded from https://academic.oup.com/mnras/article/350/4/1301/986038 by guest on 21 August 2022

1 INTRODUCTION

Type Ia supernovae (SNe Ia) appear to be good cosmological distance indicators and have been applied successfully in determining cosmological parameters (e.g. Ω and Λ; Riess et al. 1998; Perlmutter et al. 1999). They are believed to be thermonuclear explosions of mass-accreting white dwarfs (WDs), although the exact nature of their progenitors has remained unclear. In the most widely accepted model, the Chandrasekhar mass model, a carbon/oxygen (CO) WD accretes mass until it reaches a mass ∼1.378 $M_\odot$ (Nomoto, Thielemann & Yokoi 1984), close to the Chandrasekhar mass, and explodes as a SN Ia. One scenario in which this can occur is where a CO WD accretes mass by mass transfer from a binary companion, which may be a main-sequence (MS) star or a slightly evolved subgiant. This channel is referred to as the WD + MS channel (van den Heuvel et al. 1992; Rappaport, Di Stefano & Smith 1994; Li & van den Heuvel 1997; Langer et al. 2000). Here the binary system originally consists of two MS stars, where the more massive star evolves to become a CO WD by binary interactions. Subsequently, when the companion has evolved sufficiently, it starts to fill its Roche lobe and to transfer hydrogen-rich material on to the WD. The accreted hydrogen is burned into helium, and then the helium is converted to carbon and oxygen. The CO WD increases its mass until the mass reaches ∼1.378 $M_\odot$ when it explodes in a thermonuclear supernova. Whether the WD can grow in mass depends crucially on the mass-transfer rate and the evolution of the mass-transfer rate with time. If it is too high, the system may enter into a common-envelope (CE) phase (Paczyński 1976); if it is too low, burning is unstable and leads to nova explosions where all the accreted matter is ejected.

Hachisu et al. (1999a, hereafter HKNU99), Hachisu, Kato & Nomoto (1999b, hereafter HKN99) and Nomoto et al. (1999) have studied the WD + MS channel for various metallicities. However, their approach was based on a simple analytical method for treating the binary interactions. It is well established (e.g. Langer et al. 2000) that such analytical prescriptions cannot describe certain mass-transfer phases, in particular those occurring on a thermal time-scale, appropriately. Li & van den Heuvel (1997) studied this channel (for a metallicity $Z = 0.02$) with detailed binary evolution calculations, but only for two WD masses, 1.0 and 1.2 $M_\odot$, while Langer et al. (2000) investigated the channel (for metallicities $Z = 0.02$ and 0.001) considering case A evolution only (where mass transfer occurs during core hydrogen burning).

The purpose of this paper is to study the binary channel more comprehensively and to determine the detailed parameter range in which this channel produces SNe Ia, which can be used for population synthesis studies (also see Ivanova & Taam 2003). Employing the Eggleton stellar evolution code with the latest input physics, we

★E-mail: zhanwen@public.km.yn.cn

© 2004 RAS

construct a fine grid of binary models for a Population I (Pop I) metallicity $Z = 0.02$ in Sections 2 and 3, and then implement the results in a binary population synthesis (BPS) study in Section 4. In Section 5 we discuss the results and compare them to previous studies, and finally in Section 6 we summarize the main results.

2 BINARY EVOLUTION CALCULATIONS

In the WD + MS channel, the lobe-filling star is a MS star or a star not evolved far away from the MS. The star transfers some of its mass on to the WD, which grows in mass as a consequence. To determine whether the WD reaches the critical mass for a SN Ia, taken to be 1.378 $\mathrm{M}_\odot$,[1] it is necessary to perform detailed binary evolution calculations. Here we use the stellar evolution code of Eggleton (1971, 1972, 1973), modified to incorporate the WD accretion prescription of HKNU99 into the binary calculations (for an alternative prescription see Prialnik & Kovetz 1995).

The Eggleton stellar evolution code has been updated with the latest input physics over the last three decades, as described by Han, Podsiadlowski & Eggleton (1994) and Pols et al. (1995, 1998). Roche lobe overflow (RLOF) is also treated within the code (Han, Tout & Eggleton 2000). In our calculations, we use a typical Pop I composition with hydrogen abundance $X = 0.70$, helium abundance $Y = 0.28$ and metallicity $Z = 0.02$. We set $\alpha = l/H_\mathrm{p}$, the ratio of typical mixing length to the local pressure scaleheight, to 2, and set the convective overshooting parameter δ_ov to 0.12 (Pols et al. 1997; Schröder, Pols & Eggleton 1997), which roughly corresponds to an overshooting length of $\sim$0.25 pressure scaleheights (H_p).

We do not calculate the effects of accretion on to the WD explicitly, i.e. we do not solve the stellar structure equations for the WD. Instead, we adopt the prescription of HKNU99 for the growth of the mass of a CO WD by accretion of hydrogen-rich material from its companion. The prescription is given below. If the mass-transfer rate is above a critical rate, $\dot{M}_\mathrm{cr}$, we assume that hydrogen burns steadily on the surface of the WD and that the hydrogen-rich matter is converted into helium at a rate $\dot{M}_\mathrm{cr}$, while the unprocessed matter is assumed to be lost from the system, presumably in the form of an optically thick wind. The mass-loss rate of the wind is therefore $\dot{M}_\mathrm{wind} = |\dot{M}_2| - \dot{M}_\mathrm{cr}$, where $\dot{M}_2$ is the mass-transfer rate. The critical mass-transfer rate is given by

$$\dot{M}_\mathrm{cr} = 5.3 \times 10^{-7} \frac{(1.7 - X)}{X}(M_\mathrm{WD} - 0.4), \tag{1}$$

where X is the hydrogen mass fraction and M_WD is the mass of the WD (masses are in solar units and mass-accretion/transfer rates in $\mathrm{M}_\odot\ \mathrm{yr}^{-1}$). If the mass-transfer rate is less than $\dot{M}_\mathrm{cr}$ but higher than $\dot{M}_\mathrm{st} = \frac{1}{2}\dot{M}_\mathrm{cr}$, it is assumed that there is no mass loss and that hydrogen-shell burning is steady. If the mass-transfer rate is below $\frac{1}{2}\dot{M}_\mathrm{cr}$ but higher than $\frac{1}{8}\dot{M}_\mathrm{cr}$, hydrogen-shell burning is unstable, triggering very weak shell flashes, where it is assumed that the processed mass can be retained. If the mass-transfer rate is lower than $\dot{M}_\mathrm{low} = \frac{1}{8}\dot{M}_\mathrm{cr}$, hydrogen-shell flashes are so strong that no mass can be accumulated by the WD. Therefore, the growth rate of the mass of the helium layer on top of the CO WD can be written as

$$\dot{M}_\mathrm{He} = \eta_\mathrm{H}|\dot{M}_2|, \tag{2}$$

where

$$\eta_\mathrm{H} = \begin{cases} \dot{M}_\mathrm{cr}/|\dot{M}_2|, & |\dot{M}_2| > \dot{M}_\mathrm{cr}, \\ 1, & \dot{M}_\mathrm{cr} \geqslant |\dot{M}_2| \geqslant \dot{M}_\mathrm{low}, \\ 0, & |\dot{M}_2| < \dot{M}_\mathrm{low}. \end{cases} \tag{3}$$

When the mass of the helium layer reaches a certain value, helium is assumed to be ignited. If helium-shell flashes occur, a part of the envelope mass is assumed to be blown off. The mass accumulation efficiency for helium-shell flashes according to HKNU99 is given by

$$\eta_\mathrm{He} = \begin{cases} -0.175(\log \dot{M}_\mathrm{He} + 5.35)^2 + 1.05, & \\ \qquad -7.3 < \log \dot{M}_\mathrm{He} < -5.9, & \\ 1, \qquad -5.9 \leqslant \log \dot{M}_\mathrm{He} \leqslant -5. & \end{cases} \tag{4}$$

The growth rate of the CO WD is then given by $\dot{M}_\mathrm{CO}$, i.e.

$$\dot{M}_\mathrm{CO} = \eta_\mathrm{He}\dot{M}_\mathrm{He} = \eta_\mathrm{He}\eta_\mathrm{H}|\dot{M}_2|. \tag{5}$$

We assume that the mass lost from the system carries away the same specific orbital angular momentum as the WD.

These prescriptions have been incorporated into our stellar evolution code and allow us to follow the evolution of both the donor and the accreting CO WD. Altogether, we have calculated the evolution of 2298 CO WD binary systems, thus obtaining a large, dense model grid. The initial masses, M_2^i, of donor stars range from 1.5 to 4.0 $\mathrm{M}_\odot$; the initial masses, M_WD^i, of the CO WDs from 0.67 to 1.2 $\mathrm{M}_\odot$; the initial orbital periods, P^i, of the binaries from the minimum period, at which a zero-age main-sequence (ZAMS) star would fill its Roche lobe, to $\sim$30 d.

3 BINARY EVOLUTION RESULTS

In Fig. 1 we present three representative examples of our binary evolution calculations and one extreme example. It shows the mass-transfer rate, $\dot{M}_2$, the growth rate of the CO WD, $\dot{M}_\mathrm{CO}$, the mass of the CO WD, M_WD, the evolutionary track of the donor star in the Hertzsprung–Russell (HR) diagram and the evolution of the orbital period. Figs 1(a) and (b) represent the evolution of a binary system with an initial mass of the donor star of $M_2^\mathrm{i} = 2.00\ \mathrm{M}_\odot$, an initial mass of the CO WD of $M_\mathrm{WD}^\mathrm{i} = 0.75\ \mathrm{M}_\odot$ and an initial orbital period of $\log(P^\mathrm{i}\ \mathrm{d}^{-1}) = 0.20$. The donor star fills its Roche lobe on the MS which results in case A RLOF. The mass-transfer rate exceeds $\dot{M}_\mathrm{cr}$ soon after the onset of RLOF, leading to a wind phase, where part of the transferred mass is blown off in an optically thick wind, while the rest is accumulated by the WD. When the mass-transfer rate drops below $\dot{M}_\mathrm{cr}$ but is still higher than $\dot{M}_\mathrm{st}$, the optically thick wind stops and hydrogen-shell burning is stable. The mass-transfer rate decreases further to below $\dot{M}_\mathrm{st}$ but remains above $\dot{M}_\mathrm{low}$, where hydrogen-shell burning is unstable, triggering very weak shell flashes, and the WD continues to grow in mass. When the mass reaches $M_\mathrm{WD}^\mathrm{SN} = 1.378\ \mathrm{M}_\odot$, the WD is assumed to explode as a SN Ia. At this point, the mass of the donor is $M_2^\mathrm{SN} = 1.1356\ \mathrm{M}_\odot$ and the orbital period $\log(P^\mathrm{SN}\ \mathrm{d}^{-1}) = -0.0975$.

Figs 1(c) and (d) show another example for an initial system with $M_2^\mathrm{i} = 2.20\ \mathrm{M}_\odot$, $M_\mathrm{WD}^\mathrm{i} = 0.80\ \mathrm{M}_\odot$ and $\log(P^\mathrm{i}\ \mathrm{d}^{-1}) = 0.40$. The binary evolves in a similar way as in the previous example and the binary parameters, when the WD reaches $M_\mathrm{WD} = 1.378\ \mathrm{M}_\odot$, are $M_2^\mathrm{SN} = 0.8055\ \mathrm{M}_\odot$ and $\log(P^\mathrm{SN}\ \mathrm{d}^{-1}) = 0.1614$. The main difference between this example and the previous one is that RLOF

[1] Note that this means in this work we did not consider the possible effects of rotation, which, as shown by Yoon & Langer (2002), may significantly increase the critical explosion mass for a CO WD above the standard Chandrasekhar limit of $\sim$1.4 $\mathrm{M}_\odot$. The calculations of Yoon, Langer & Scheithauer (2004) also show that helium burning is much less violent when rotation is taken into account; this may significantly increase the accretion efficiency (i.e. η_He in our parametrization).

Downloaded from https://academic.oup.com/mnras/article/350/4/1301/986038 by guest on 21 August 2022

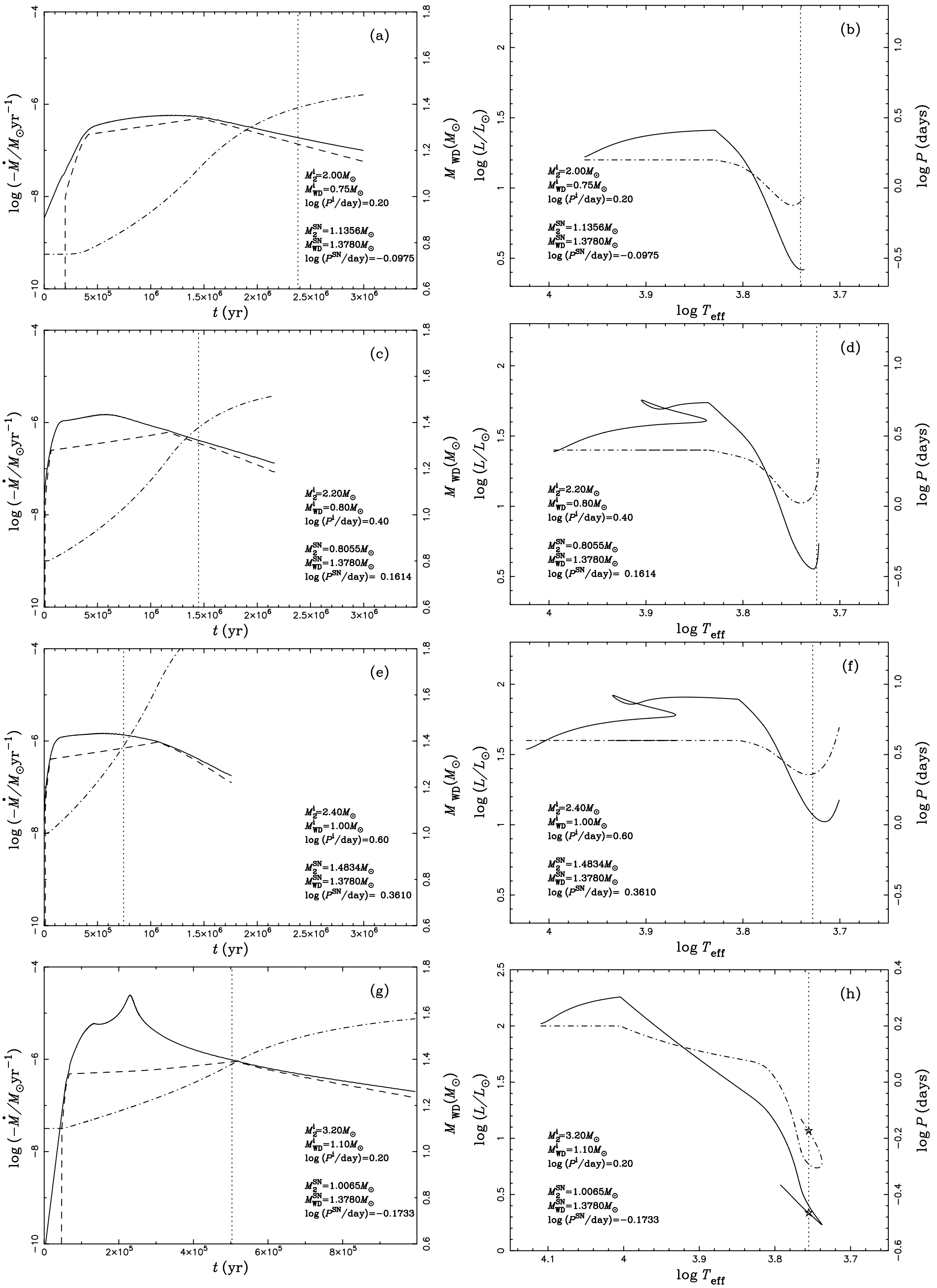

Figure 1. Three representative examples of binary evolution calculations and one extreme example. The solid, dashed and dash-dotted curves show the mass-transfer rate, $\dot{M}_2$, the mass-growth rate of the CO WD, $\dot{M}_{\rm CO}$, the mass of the CO WD, $M_{\rm WD}$, respectively, in panels (a), (c), (e) and (g). The evolutionary tracks of the donor stars are shown as solid curves and the evolution of orbital period is shown as dash-dotted curves in panels (b), (d), (f) and (h). Dotted vertical lines in all panels and asterisks in panel (h) indicate the position where the WD is expected to explode in a SN Ia. The initial binary parameters and the parameters at the time of the SN Ia explosion are also given in each panel.

begins in the Hertzsprung gap (i.e. after the secondary has left the MS; so-called early case B evolution) and that, at the time of the explosion, the system is still in the stable hydrogen-burning phase after the optically thick wind phase.

The third example in Figs 1(e) and (f) represents the case where mass transfer starts in the Hertzsprung gap and where the binary remains in the optically thick phase even at the supernova stage. In this case, the initial binary parameters are $M_2^{\rm i} = 2.40\ {\rm M}_{\odot}$, $M_{\rm WD}^{\rm i} =$

Downloaded from https://academic.oup.com/mnras/article/350/4/1301/986038 by guest on 21 August 2022

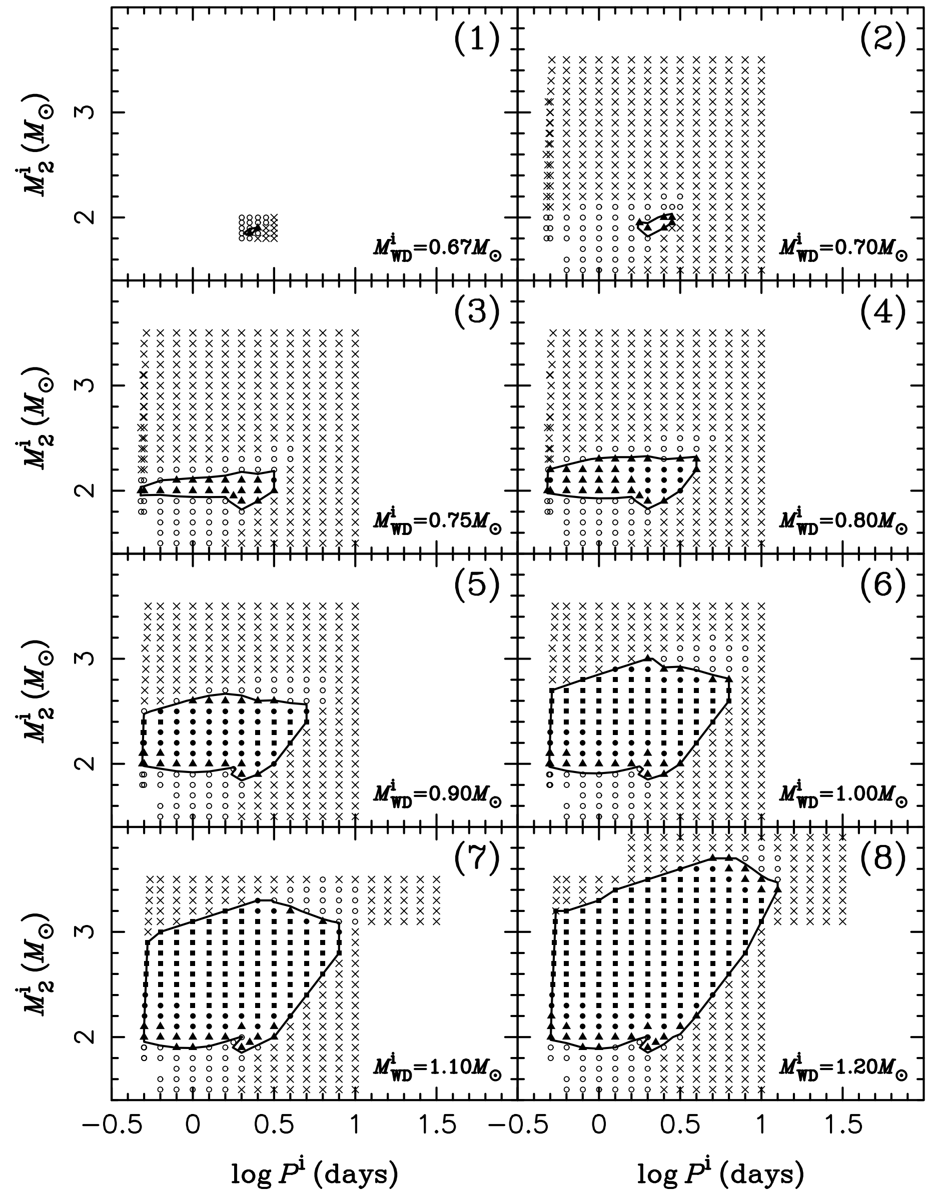

Figure 2. Final outcomes of the binary evolution calculations in the initial orbital period–secondary mass ($\log P^{\rm i}$, $M_2^{\rm i}$) plane of the CO + MS binary, where $P^{\rm i}$ is the initial orbital period and $M_2^{\rm i}$ is the initial mass of the donor star (for different initial WD masses as indicated in each panel). Filled squares indicate SN Ia explosions during an optically thick wind phase ($|\dot{M}_2| \geqslant \dot{M}_{\rm cr}$). Filled circles denote SN Ia explosions after the wind phase, where hydrogen-shell burning is stable ($\dot{M}_{\rm cr} > |\dot{M}_2| \geqslant \dot{M}_{\rm cr}$). Filled triangles denote Ia explosions after the wind phase where hydrogen-shell burning is mildly unstable ($\dot{M}_{\rm st} > |\dot{M}_2| \geqslant \dot{M}_{\rm low}$). Open circles indicate systems that experience novae, preventing the WD from reaching 1.378 M$_\odot$, while crosses show systems that are unstable to dynamical mass transfer.

1.00 M$_\odot$ and $\log (P^{\rm i}\ {\rm d}^{-1}) = 0.60$. When $M_{\rm WD} = 1.378$ M$_\odot$, they are $M_2^{\rm SN} = 1.4834$ M$_\odot$ and $\log (P^{\rm SN}\ {\rm d}^{-1}) = 0.3610$.

Finally, Figs 1(g) and (h) illustrate a more extreme case where both the donor and the WD are relatively massive. The initial binary parameters in this case are $M_2^{\rm i} = 3.30$ M$_\odot$, $M_{\rm WD}^{\rm i} = 1.10$ M$_\odot$ and $\log (P^{\rm i}\ {\rm d}^{-1}) = 0.20$. The donor loses ∼0.5 M$_\odot$ in the first 1.8×10^5 yr after the onset of RLOF; at this stage mass transfer becomes almost dynamically unstable and hence the mass-transfer rate increases sharply, only to drop once the mass ratio has been reversed. The binary parameters at the explosion are $M_2^{\rm SN} = 1.0065$ M$_\odot$ and $\log (P^{\rm SN}\ {\rm d}^{-1}) = -0.1733$. For an even larger initial donor mass, e.g. $M_2^{\rm i} = 3.40$ M$_\odot$, our calculations show that mass transfer becomes unstable, and such systems experience a delayed dynamical instability (Hjellming & Webbink 1987).

Fig. 2 summarizes the final outcome of the 2298 binary evolution calculations in the initial orbital period–secondary mass ($\log P^{\rm i}$, $M_2^{\rm i}$) plane. Filled symbols show that the evolution leads to a SN Ia, where the shape of the symbols indicates whether the WD explodes in the optically thick wind phase (filled squares: $|\dot{M}_2| \geqslant \dot{M}_{\rm cr}$), after the wind phase in the stable hydrogen-burning phase (filled circles: $\dot{M}_{\rm cr} > |\dot{M}_2| \geqslant \dot{M}_{\rm cr}$) or in the unstable hydrogen-shell burning phase (filled triangles: $\dot{M}_{\rm st} > |\dot{M}_2| \geqslant \dot{M}_{\rm low}$). Systems which experience nova explosions and never reach the Chandrasekhar limit and systems that may experience a CE phase are also indicated in the figure.

In Figs 2 and 3 we also present the contours for the initial parameters for which a SN Ia results. The left boundaries of these contours in Fig. 2 (panels 3–8) are set by the condition that RLOF starts when the secondary is still unevolved (i.e. is on the ZAMS),

Downloaded from https://academic.oup.com/mnras/article/350/4/1301/986038 by guest on 21 August 2022

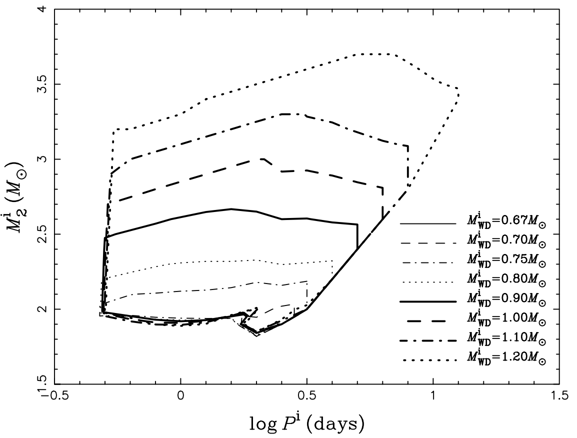

Figure 3. Regions in the initial orbital period–secondary mass plane (log $P^{\rm i}$, $M^{\rm i}_2$) for WD binaries that produce SNe Ia for initial WD masses of 0.67, 0.70, 0.75, 0.80, 0.90, 1.0, 1.1 and 1.2 $\mathrm{M}_\odot$. The region almost vanishes for $M^{\rm i}_{\rm WD} = 0.67\ \mathrm{M}_\odot$.

while systems beyond the right boundary are systems that experience dynamically unstable mass transfer when mass transfer starts at the base of the red giant branch (RGB). The upper boundaries are also mainly set by the condition of dynamical stability, because systems above the boundary have too large a mass ratio for stable mass transfer. The lower boundaries are caused by the constraints that the mass-transfer rate has to be high enough for the WD to be able to grow and that the donor mass is sufficiently massive that enough mass can be transferred to the WD for it to be able to reach the Chandrasekhar limit. SNe Ia are either produced through case A binary evolution (the left parts of the regions), where hydrogen burning occurs in the centre of the donor star at the onset of RLOF, or early case B binary evolution (the right parts of the regions), where hydrogen has already been exhausted in the centre and the donor is in the Hertzsprung gap at the onset of the RLOF phase.

In Fig. 3, we overlay the contours for SN Ia production in the (log $P^{\rm i}$, $M^{\rm i}_2$) plane for initial WD masses of 0.67, 0.70, 0.75, 0.80, 0.90, 1.0, 1.1 and 1.2 $\mathrm{M}_\odot$. Note that the enclosed region almost vanishes for $M^{\rm i}_{\rm WD} = 0.67\ \mathrm{M}_\odot$, which therefore sets the minimum WD mass for which this channel can produce a supernova. In Appendix A, we present fitting formulae for the boundaries of these contours (accurate to 3 per cent for most boundaries), which can be used for population synthesis studies. If the initial parameters of a CO WD binary system are located in the SN Ia production region, a SN Ia is assumed to be the outcome of the binary evolution.

4 BINARY POPULATION SYNTHESIS

In order to estimate the supernova frequencies in the WD + MS channel, we first need to determine the distribution and properties of CO WD binaries. There are two channels to produce such systems. In the first, the primary is in a relatively wide binary and fills its Roche lobe as an asymptotic giant, where mass transfer is dynamically unstable. This leads to the formation of a CE phase (Paczyński 1976) and the spiral-in of the core of the giant and the secondary inside this envelope (due to friction with the CE). If the orbital energy released in the orbital decay is able to eject the envelope, this produces a rather close binary consisting of the WD core of the primary (here, a CO WD) and the secondary. As is usually done in BPS studies, we assume that the CE is ejected if

$$\alpha_{\rm CE}\Delta E_{\rm orb} \geqslant |E_{\rm bind}|, \tag{6}$$

where $\Delta\ E_{\rm orb}$ is the orbital energy released, $E_{\rm bind}$ is the binding energy of the envelope, and $\alpha_{\rm CE}$ is the CE ejection efficiency, i.e. the fraction of the released orbital energy used to overcome the binding energy. We adopt $E_{\rm bind} = E_{\rm gr} - \alpha_{\rm th} E_{\rm th}$, where $E_{\rm gr}$ is the gravitational binding energy, $E_{\rm th}$ is the thermal energy, and $\alpha_{\rm th}$ defines the fraction of the thermal energy contributing to the CE ejection.

A second channel to produce close CO WD binary systems involves so-called case BB binary evolution (Delgado & Thomas 1981), where the primary fills its Roche lobe when it has a helium core, leaving a helium star at the end of the first RLOF phase. After it has exhausted the helium in the core, the helium star, now containing a CO core, expands and fills its Roche lobe again, transferring its remaining helium-rich envelope, producing a CO WD binary in the process.

The CO WD binary system continues to evolve, and the secondary will at some point also fill its Roche lobe; the WD will then start to accrete mass from the secondary and convert the accreted matter into CO. We assume that this ultimately produces a SN Ia if, at the beginning of this RLOF phase, the orbital period, $P^{\rm i}_{\rm orb}$, and secondary mass, $M^{\rm i}_2$, are in the appropriate regions in the (log $P^{\rm i}$, $M^{\rm i}_2$) plane (see Fig. 3) to produce a SN Ia.

In order to investigate the birth rates of SNe Ia, we have performed a series of detailed Monte Carlo simulations with the latest version of the BPS code developed by Han et al. (2003). In each simulation, we follow the evolution of 100 million sample binaries according to grids of stellar models of metallicity $Z = 0.02$ and the evolution channels described above. We adopt the following input for the simulations (see Han, Podsiadlowski & Eggleton 1995, for details). (1) The star formation rate (SFR) is taken to be constant over the last 15 Gyr or, alternatively, as a delta function, i.e. a single starburst. In the case of a constant SFR, we assume that a binary with its primary more massive than 0.8 $\mathrm{M}_\odot$ is formed annually. For the case of a single starburst, we assume a burst producing $10^{11}\ \mathrm{M}_\odot$ in stars. (2) The initial mass function (IMF) of Miller & Scalo (1979) is adopted. (3) The mass-ratio distribution is taken to be constant or, alternatively, it is assumed that the component masses are uncorrelated. (4) We take the distribution of separations to be constant in $\log a$ for wide binaries, where a is the orbital separation. Our adopted distribution implies that ~50 per cent of stellar systems are binary systems with orbital periods less than 100 yr.

The results of the simulations are plotted in Figs 6–9.

5 DISCUSSION

5.1 Comparisons with previous studies

Langer et al. (2000) investigated the CO + MS channel for SNe Ia considering case A evolution for metallicities $Z = 0.02$ and $Z = 0.001$, respectively, where they used a simple prescription for the WD mass accretion. We checked that we obtain very similar results, e.g. similar mass-transfer rates, similar final WD masses, if we adopt similar prescriptions. They also pointed out the possibility that binary systems where the WD has an initial mass as small as ~0.7 $\mathrm{M}_\odot$ can produce a SNe Ia. This agrees with our results which show that binary systems with $M^{\rm i}_{\rm WD} = 0.67\ \mathrm{M}_\odot$ can lead to a SN Ia. However, their upper limit for donor stars of 2.3 $\mathrm{M}_\odot$ in the progenitor binaries is substantially smaller than the limit of 3.7 $\mathrm{M}_\odot$ found in this study. There are several reasons for this difference. First, the upper limit of 2.3 $\mathrm{M}_\odot$ in Langer et al. (2000) arises from

Downloaded from https://academic.oup.com/mnras/article/350/4/1301/986038 by guest on 21 August 2022

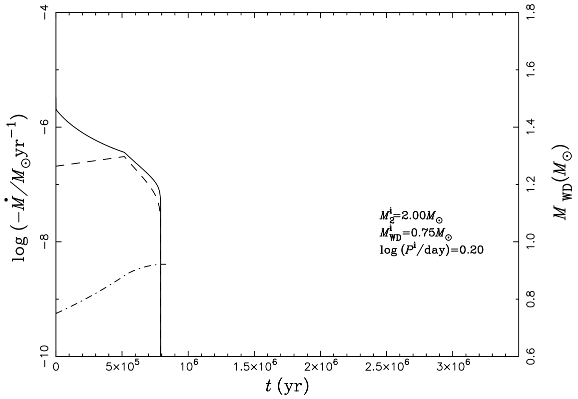

Figure 4. The evolution of mass-transfer rate, $\dot{M}_2$, mass-growth rate of the CO WD, $\dot{M}_{\rm CO}$, and the CO WD mass, $M_{\rm WD}$, similar to panel (a) of Fig. 1, but using an analytical approach similar to that of HKNU99 rather than detailed binary calculations.

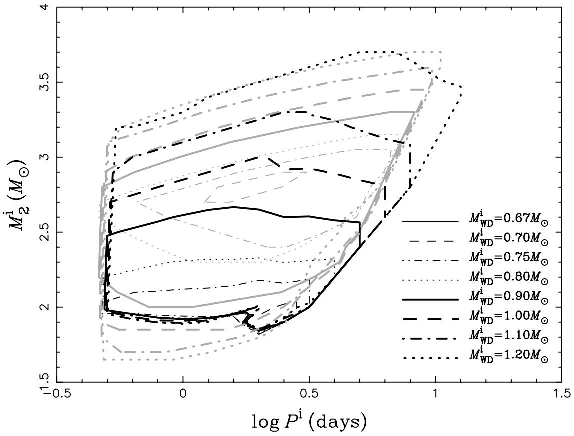

Figure 5. A comparison of the results of this paper with those obtained by HKNU99 and HKN99. Dark contours show the parameter regions in the $(\log P, \log M_2^{\rm i})$ plane for different WD masses that lead to a SN Ia. The light grey contours are taken from HKN99 and HKNU99.

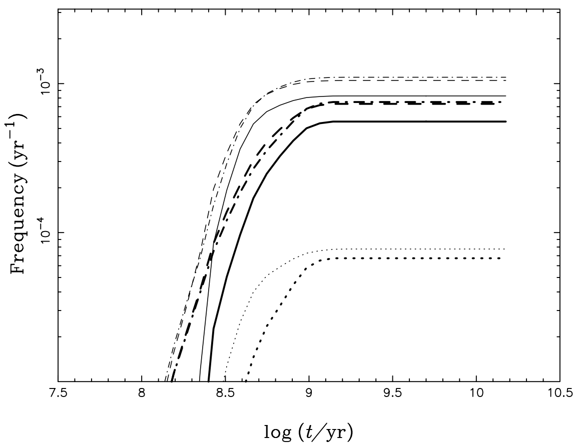

Figure 6. The evolution of birth rates of SNe Ia for a constant Pop I SFR (3.5 M$_\odot$ yr^{-1}). Solid, dashed and dash-dotted curves are for a constant initial mass-ratio distribution and with $\alpha_{\rm CE} = \alpha_{\rm th} = 1.0$ (solid), 0.75 (dashed) and 0.5 (dash-dotted), respectively. Dotted curves are with $\alpha_{\rm CE} = \alpha_{\rm th} = 1.0$ and for a mass-ratio distribution with uncorrelated component masses. Thick curves are based on the contours in this paper, while thin curves are based on the results of HKNU99.

a progenitor binary with $M_{\rm WD}^{\rm i} = 1.0$ M$_\odot$, while ours occurs in a system with $M_{\rm WD}^{\rm i} = 1.2$ M$_\odot$. This increases the maximum mass of the companion for which mass transfer remains stable. Secondly, Langer et al. (2000) limited the maximum possible wind mass-loss rate to three times the Eddington limit of the accreting WD. Thirdly, they only considered case A mass transfer, while we did not limit the mass-loss rate[2] and considered both case A and case B evolution.

Li & van den Heuvel (1997) studied the evolution of WD binaries in search for progenitors of SNe Ia by using assumptions similar to those of Hachisu, Kato & Nomoto (1996), HKN99 and HKNU99, but only for two WD masses, 1.0 and 1.2 M$_\odot$. Our contours for the regions of WD binaries producing SNe Ia are consistent with theirs if we take into account that their model grid is much smaller and that their stellar evolution model parameters (e.g. overshooting parameter) may be different from ours.

HKNU99, HKN99 and Nomoto et al. (1999) studied the WD + MS channel for progenitors of SNe Ia with different metallicities. They used the analytical fitting formulae of Tout et al. (1997) to calculate the radius and the luminosity of a MS star. As the mass transfer proceeds on a thermal time-scale for $M_2^{\rm i}/M_{\rm WD}^{\rm i} > 0.79$, they approximated the mass-transfer rate as

$$|\dot{M}_2| = \frac{M_2}{\tau_{\rm KH}}{\rm Max}\left(\frac{\zeta_{\rm RL} - \zeta_{\rm MS}}{\zeta_{\rm MS}}, 0\right) \qquad (7)$$

where $\tau_{\rm KH}$ is the Kelvin–Helmholtz time-scale, and $\zeta_{\rm RL}$ and $\zeta_{\rm MS}$ are the mass-radius exponents of the inner critical Roche lobe and the MS star, respectively. In order to be able to make a comparison, we adopted a similar approach to calculate the evolution of a binary system with initial parameters $M_2^{\rm i} = 2.00$ M$_\odot$, $M_{\rm WD}^{\rm i} = 0.75$ M$_\odot$ and $\log\,(P^{\rm i}\ {\rm d}^{-1}) = 0.20$, the results of which are shown in Fig. 4. Comparison of Fig. 4 and Fig. 1(a) shows that the estimate of the mass-transfer rate is significantly different in this model compared to the results of our detailed binary calculations (also see Langer et al. 2000, for a detailed analysis). The estimated mass-transfer rate is significantly larger, and the mass-transfer phase is correspondingly much shorter. The contours of HKNU99 are plotted as light grey curves in Fig. 5. Our contours are similar to theirs for massive WDs, but very different for low-mass WDs. For example, the contour for $M_{\rm WD}^{\rm i} = 0.75$ M$_\odot$ in HKNU99 corresponds to significantly more massive donors ($\sim$2.7 M$_\odot$) than our contour ($\sim$2.0 M$_\odot$). The enclosed region of the contour of HKNU99 is also larger. We consider our contours more physical as they are based on detailed binary evolution calculations rather than a simple prescription for estimating the mass-transfer rate and use the latest stellar evolution physics.

5.2 Birth rates of SNe Ia

Fig. 6 shows Galactic birth rates of SNe Ia for the WD + MS channel. The simulations for a constant initial mass-ratio distribution give a Galactic birth rate of 0.6–1.1 $\times$ 10^{-3} yr^{-1}, lower but not dramatically lower than the birth rate inferred observationally (i.e. within a factor of a few, 3–4 $\times$ 10^{-3} yr^{-1}; van den Bergh &

[2] In this context, we note that observations of some neutron star/black hole binaries provide observational evidence that these systems can lose mass from the binary system at rates that exceed the Eddington accretion rate of the compact object by several orders of magnitude, e.g. Cyg X-2 (King & Ritter 1999; Podsiadlowski & Rappaport 2000) and SS 433 (Blundell et al. 2001).

Downloaded from https://academic.oup.com/mnras/article/350/4/1301/986038 by guest on 21 August 2022

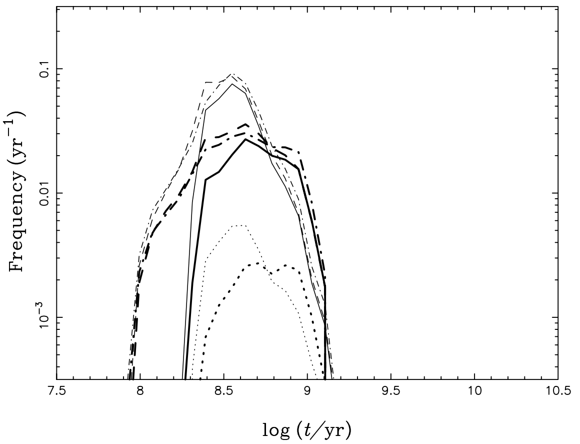

Figure 7. Similar to Fig. 6, but for a single starburst of 10^{11} M$_\odot$.

Tammann 1991; Cappellaro & Turatto 1997). The simulation for the initial mass-ratio distribution with uncorrelated component masses gives a birth rate that is lower by an order of magnitude, as most of the donors in the WD + MS channel are not very massive which has the consequence that the WDs cannot accrete enough mass to reach the Chandrasekhar limit. The birth rates based on our new contours (Fig. 3) are 0.6–0.8 × 10^{-3} yr^{-1}, lower than the birth rates one would obtain with the contours of HKNU99 for a constant mass-ratio distribution (0.8–1.1 × 10^{-3} yr^{-1}). This follows directly from the fact that the parameter regions where low-mass WDs can produce a SN Ia is smaller in our study than in HKNU99 (see Fig. 5).

Yungelson & Livio (1998) gave a much lower SN Ia birth rate for the WD + MS channel, which is just 10 per cent of the inferred SN Ia rate. HKN99 speculated that an important evolutionary path (case BB evolution) was not included in the model of Yungelson & Livio (1998). However, Yungelson (private communication) has since pointed out that case BB evolution was indeed included, although not mentioned specifically. The difference is most likely due to the fact that they based the efficiency for hydrogen accumulation on Prialnik & Kovetz (1995), which is significantly lower than the efficiency assumed in this study (see also Fedorova, Tutukov & Yungelson 2004). In addition, their treatment of CE evolution is also quite different (see the discussion of Han et al. 1995).

HKN99 proposed a wide symbiotic channel (i.e. WD + RG channel, in which a low-mass red giant is the mass donor) to increase the number of possible SN Ia progenitors and gave the corresponding regions in the (log $P^{\rm i}$, $M_2^{\rm i}$) plane. However, at present it is not clear from a BPS point of view how to populate this parameter region with WD systems. Our BPS model would predict that the Galactic SN Ia rate from the WD + RG channel is negligible (∼2 × 10^{-5} yr^{-1}). This is consistent with the conclusions of Yungelson & Livio (1998). On the other hand, several recurrent novae are known to exist in this parameter region (e.g. HKN99); this may suggest a problem with some of the assumptions in the BPS model, an issue that needs to be investigated further.

Fig. 7 displays the evolution of birth rates of SNe Ia for a single starburst of 10^{11} M$_\odot$. Most of the supernova explosions occur between 0.1 and 1 Gyr after the burst. The figure also shows that a high CE ejection efficiency leads to a systematically later explosion time, because a high CE ejection efficiency leads to wider WD binaries, and, as a consequence, it takes a longer time for the secondary to evolve to fill its Roche lobe. A high upper limit for the donor mass in Fig. 3, on the other hand, would result in an earlier explosion time, as the evolutionary time-scale is shorter for a massive donor. The SN Ia rate would also be higher, although by not much, as the SN Ia production region in Fig. 3 becomes bigger.

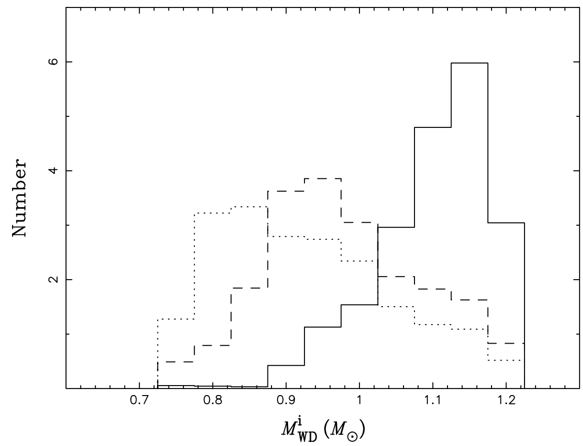

Figure 8. The distribution of the initial masses of the CO WDs for the progenitors of SNe Ia as determined from the results of this study. The solid, dashed and dotted histograms are for SNe Ia produced at 0.3, 0.5 and 0.7 Gyr after a single starburst. The simulation uses a metallicity $Z = 0.02$, a constant initial mass-ratio distribution and $\alpha_{\rm CE} = \alpha_{\rm th} = 1.0$.

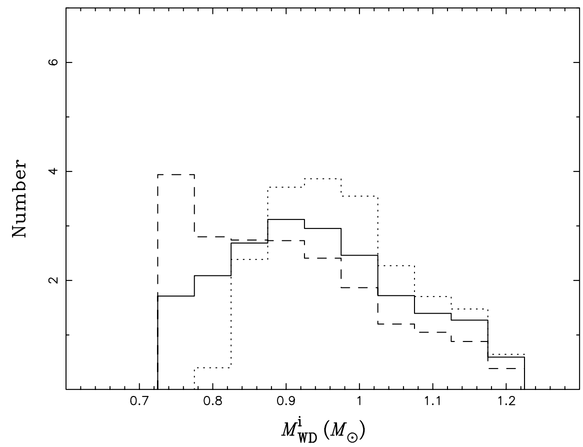

Figure 9. Similar to Fig. 8, but based on the results of HKNU99.

5.3 Distribution of the initial WD masses

Fig. 8 shows the distributions of the initial masses of the CO WDs that ultimately produce a SNe Ia according to our new calculations. The distributions are shown for systems that produce SNe Ia at 0.3, 0.5 and 0.7 Gyr after a single starburst. For clarity, we only show the distributions for the simulation with a constant initial mass-ratio distribution and for $\alpha_{\rm CE} = \alpha_{\rm th} = 1.0$, as the other simulations gave similar results. The figure shows that there is a clear trend for the peak in the initial WD mass distribution to move to lower masses with time, where the first SNe Ia preferentially have massive WD progenitors. Such a clear trend is not seen when the contours of HKNU99 are used (Fig. 9). Here the trend is not so clear, and the peak moves first to lower mass and subsequently to higher mass as the age increases. The difference between Figs 8 and 9 can be entirely understood from the different behaviour of the contours in the two studies and the fact that a massive donor in the WD + MS channel will evolve more quickly and hence produce a supernova at an earlier time.

Downloaded from https://academic.oup.com/mnras/article/350/4/1301/986038 by guest on 21 August 2022

The brightness of a SN Ia is mainly determined by the mass of ^{56}Ni synthesized ($M_{\rm Ni}$) during the explosion. As pointed out by Höflich, Wheeler & Thielemann (1998) and Nomoto et al. (1999), the amount of ^{56}Ni synthesized will generally depend on the C/O ratio in the core of the WD just before the explosion. Nomoto et al. (1999) speculated that the supernova brightness increases with the C/O ratio. We tested the C/O relation with mass in our stellar evolution code and found, in agreement with earlier studies, that the C/O ratio decreases with increasing ZAMS mass and hence WD mass. This would suggest that older progenitors, which tend to have lower initial WD mass (Fig. 6), should produce brighter SNe Ia in the WD + MS channel. However, irrespective of what the correlation of the C/O ratio with explosion energy may be, it is clear that the C/O ratio is important in determining the explosion energy. Because the C/O ratio depends on the age of the population and also the metallicity (see Höflich et al. 1998 and Langer et al. 2000, for further discussions), this may introduce evolutionary effects that may need to be taken into account in cosmological applications of SNe Ia.

Nomoto et al. (1999) have studied the distribution of the initial WD masses both for the WD + MS channel and the WD + RG channel. They found that the WD + RG channel tends to have larger WD masses on average as a more massive WD is generally needed to allow stable RLOF (rather than lead to dynamical mass transfer and a CE phase). As a consequence, SNe Ia from the WD + RG channel would tend to be dimmer (assuming the above relation between supernova brightness and C/O ratio/WD mass). At an age of 10 Gyr, the WD + RG channel is the major single-degenerate channel to produce SNe Ia. This could explain why SNe Ia are much dimmer in elliptical galaxies. In our BPS simulations, the WD + RG channel was not important (see the earlier discussion), and the WD + MS channel alone cannot explain the SNe Ia in elliptical galaxies. An alternative, arguably much less attractive alternative, is that the theoretically less favoured double-degenerate (DD) channel for SNe Ia (Iben & Tutukov 1984; Webbink & Iben 1987), in which two CO WDs with a total mass larger than the Chandrasekhar mass limit coalesce, may be required in old populations (Han 1998; Yungelson & Livio 1998, 2000; Tutukov & Yungelson 2002).

Finally, Langer et al. (2000) and Nomoto et al. (1999) pointed out that a more massive WD is needed to produce a SN Ia at low metallicity. As a low metallicity is in some sense similar to a young age from a stellar evolution point of view, this implies that the SNe Ia in low-metallicity populations should be dimmer.

6 SUMMARY AND CONCLUSION

Adopting the prescription of HKNU99 for the mass accretion of CO WDs, we have carried out detailed binary evolution calculations for the progenitors of SNe Ia in the single-degenerate channel (the WD + MS channel) and obtained the initial parameters in the (log $P^{\rm i}$, $M_2^{\rm i}$) plane that lead to SNe Ia. We have provided fitting formulae that give the contours for the initial binary parameters that can be used in BPS studies. We find that a CO WD with its mass as low as 0.67 $\rm M_{\odot}$ can accrete mass and reach the Chandrasekhar mass limit. By incorporating the contours into our BPS code, we obtained the birth rates of SNe Ia and their evolution with time. The Galactic birth rate is lower than but still comparable within a factor of a few to that inferred observationally.

ACKNOWLEDGMENTS

We thank Professor Yungelson for useful discussions. This work was in part supported by a Royal Society UK–China Joint Project Grant (PhP and ZH), the Chinese National Science Foundation under Grant No. 19925312, the Chinese Academy of Sciences under Grant No. KJCX2-SW-T06, and NKBRSF No. 19990754 (ZH) and a European Research and Training Network on Type Ia Supernovae (HPRN-CT-20002-00303).

REFERENCES

Blundell K. M., Mioduszewski A. J., Muxlow T. W., Podsiadlowski Ph., Rupen M. P., 2001, ApJ, 562, L79
Cappellaro E., Turatto M., 1997, in Ruiz-Lapuente P., Canal R., Isern J., eds,, Thermonuclear Supernovae. Kluwer, Dordrecht, p. 77
Delgado A. J., Thomas H. C., 1981, A&A, 96, 142
Eggleton P. P., 1971, MNRAS, 151, 351
Eggleton P. P., 1972, MNRAS, 156, 361
Eggleton P. P., 1973, MNRAS, 163, 179
Fedorova A. V., Tutukov A. V., Yungelson L. R., 2004, Astron. Lett., 30, 73
Hachisu I., Kato M., Nomoto K., 1996, ApJ, 470, L97
Hachisu I., Kato M., Nomoto K., Umeda H., 1999a, ApJ, 519, 314 (HKNU99)
Hachisu I., Kato M., Nomoto K., 1999b, ApJ, 522, 487 (HKN99)
Han Z., 1998, MNRAS, 296, 1019
Han Z., Podsiadlowski Ph., Eggleton P. P., 1994, MNRAS, 270, 121
Han Z., Podsiadlowski Ph., Eggleton P. P., 1995, MNRAS, 272, 800
Han Z., Tout C. A., Eggleton P. P., 2000, MNRAS, 319, 215
Han Z., Podsiadlowski Ph., Maxted P. F. L., Marsh T. R., 2003, MNRAS, 341, 669
Hjellming M. S., Webbink R. F., 1987, ApJ, 318, 794
Höflich P., Wheeler J. C., Thielemann F. K., 1998, ApJ, 495, 617
Iben I., Jr, Tutukov A. V., 1984, ApJS, 54, 335
Ivanova N., Taam R. E., 2003, ApJ, 601, 1058
King A. R., Ritter H., 1999, MNRAS, 309, 253
Langer N., Deutschmann A., Wellstein S., Höflich P., 2000, A&A, 362, 1046
Li X.-D., van den Heuvel E. P. J., 1997, A&A, 322, L9
Miller G. E., Scalo J. M., 1979, ApJS, 41, 513
Nomoto K., Thielemann F., Yokoi K., 1984, ApJ, 286, 644
Nomoto K., Umeda H., Hachisu I., Kato M., Kobayashi C., Tsujimoto T., 1999, in Truran J., Niemeyer J., eds, Type Ia Supernovae: Theory and Cosmology. Cambridge Univ. Press, New York, p. 63
Paczyński B., 1976, in Eggleton P. P., Mitton S., Whelan J., eds, Structure and Evolution of Close Binaries. Kluwer, Dordrecht, p. 75
Perlmutter S. et al., 1999, ApJ, 517, 565
Podsiadlowski Ph., Rappaport S., 2000, ApJ, 529, 946
Pols O. R., Tout C. A., Eggleton P. P., Han Z., 1995, MNRAS, 274, 964
Pols O. R., Tout C. A., Schröder K.-P., Eggleton P. P., Manners J., 1997, MNRAS, 289, 869
Pols O. R., Schröder K.-P., Hurley J. R., Tout C. A., Eggleton P. P., 1998, MNRAS, 298, 525
Prialnik D., Kovetz A., 1995, ApJ, 445, 789
Rappaport S., Di Stefano R., Smith J. D., 1994, ApJ, 426, 692
Riess A. et al., 1998, AJ, 116, 1009
Schröder K.-P., Pols O. R., Eggleton P. P., 1997, MNRAS, 285, 696
Tout C. A., Aarseth S. J., Pols O. R., Eggleton P. P., 1997, MNRAS, 291, 732
Tutukov A. V., Yungelson L. R., 2002, Astron. Rep., 46, 667
van den Bergh S., Tammann G. A., 1991, ARA&A, 29, 363
van den Heuvel E. P. J., Bhattacharya D., Nomoto K., Rappaport S., 1992, A&A, 262, 97
Webbink R. F., Iben I. Jr., 1987, in Philipp A. G. D., Hayes D. S., Liebert J. W., eds, IAU Colloq. 95, Second Conference on Faint Blue Stars. Davis Press, Schenectady, p. 445
Yoon S.-C., Langer N., 2002, in Hillebrandt W., Müller E., eds, Proc. 11th Workshop on Nuclear Astrophysics. MPA, Garching, p. 37
Yoon S.-C., Langer N., Scheithauer S., 2004, A&A, submitted
Yungelson L., Livio M., 1998, ApJ, 497, 168
Yungelson L., Livio M., 2000, ApJ, 528, 108

Downloaded from https://academic.oup.com/mnras/article/350/4/1301/986038 by guest on 21 August 2022

APPENDIX A: FITTING FORMULAE FOR THE BOUNDARIES OF SN IA PRODUCTION REGIONS

The upper boundaries of the contours in Fig. 3 can be fitted as

$$M_2^{\rm i} = {\rm Min}\left[A + B\log P^{\rm i} + C(\log P^{\rm i})^2 + D(\log P^{\rm i})^3, 3.2M_{\rm WD}^{\rm i}\right] \tag{A1}$$

where

$$\begin{cases} A = -1.9 + 7.078M_{\rm WD}^{\rm i} - 2.284\left(M_{\rm WD}^{\rm i}\right)^2 \\ B = -1.482 + 2.504M_{\rm WD}^{\rm i} - 0.5917\left(M_{\rm WD}^{\rm i}\right)^2 \\ C = 13.88 - 31.50M_{\rm WD}^{\rm i} + 16.86\left(M_{\rm WD}^{\rm i}\right)^2 \\ D = 1.205 + 1.243M_{\rm WD}^{\rm i} - 2.414\left(M_{\rm WD}^{\rm i}\right)^2. \end{cases} \tag{A2}$$

In the fitting we ignored the vertical parts (at the right of the upper boundaries) as they are due to the finite spacing of our model grid.

The lower and the right boundaries can be fitted as

$$M_2^{\rm i} = \begin{cases} 1.946 - 0.03261M_{\rm WD}^{\rm i} - 0.03639\log P^{\rm i} + 0.4366(\log P^{\rm i})^2 & \text{if } \log P^{\rm i} \leqslant 0.24 \\ 1.145 - 0.007195M_{\rm WD}^{\rm i} + 0.02563/(\log P^{\rm i})^2 + 1.175\log P^{\rm i} + 0.7361(\log P^{\rm i})^2 & \text{if } \log P^{\rm i} > 0.24. \end{cases} \tag{A3}$$

The left boundaries are either defined by the onset of RLOF from the secondary on the ZAMS for high-mass WDs, or by the onset of RLOF at the beginning of the Hertzsprung gap for low-mass WDs. We also carried out additional binary evolution calculations and found that, when $M_{\rm WD}^{\rm i}$ is lower than 0.73 $M_\odot$, SNe Ia cannot be produced by case A evolution. We therefore obtain

$$\log P^{\rm i} = \begin{cases} -0.4096 + 0.05301M_{\rm WD}^{\rm i} + 0.02488M_2^{\rm i}, & \text{if } M_{\rm WD}^{\rm i} \geqslant 0.73 \\ 0.24, & \text{if } M_{\rm WD}^{\rm i} < 0.73. \end{cases} \tag{A4}$$

In the above fitting formulae, the masses are in $M_\odot$ and the orbital period is in d. The formulae are valid for 0.6 $M_\odot \leqslant M_{\rm WD}^{\rm i} \leqslant$ 1.2 $M_\odot$, 1.5 $M_\odot \leqslant M_2^{\rm i} \leqslant$ 4.0 $M_\odot$ and $-0.5 \leqslant \log(P^{\rm i}\ {\rm d}^{-1}) \leqslant 1.5$. If the initial parameters of a CO WD binary system are located in the SN Ia production region, i.e. the binary is below the upper boundary (equation A1), above the lower and the right boundaries (equation A3) and to the right of the left boundary (equation A4), a SN Ia is assumed to result from the binary evolution. The formulae are written into a FORTRAN code and the code can be supplied on request by contacting ZH.

This paper has been typeset from a TEX/LATEX file prepared by the author.

Downloaded from https://academic.oup.com/mnras/article/350/4/1301/986038 by guest on 21 August 2022